Heliyon 9 (2023) e21533

Contents lists available at ScienceDirect

Heliyon

journal homepage: www.cell.com/heliyon

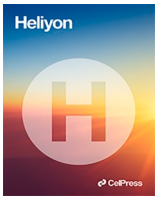

Potential investigation of combined natural dye pigments extracted from ivy gourd leaves, black glutinous rice and turmeric for dye-sensitised solar cell

V. Seithtanabutara [a,e], N. Chumwangwapee [b], A. Suksri [c,e], T. Wongwuttanasatian [b,d,e,*]

[a] Chemical Engineering Division, Faculty of Engineering, Khon Kaen University, Thailand
[b] Energy Engineering Program, Faculty of Engineering, Khon Kaen University, Thailand
[c] Electrical Engineering Division, Faculty of Engineering, Khon Kaen University, Thailand
[d] Mechanical Engineering Division, Faculty of Engineering, Khon Kaen University, Thailand
[e] Centre for Alternative Energy Research and Development, Khon Kaen University, Thailand

ARTICLE INFO

Keywords:
Dye sensitised solar cell
natural dye
UV–Visible
Absorption
Bi-colour
Performance of DSSC

ABSTRACT

Environmental sustainability, resource availability, and cost-effectiveness are the driving forces behind the search for natural sensitised dyes to replace synthetic ones. Using a combination of pigments as the sensitised dye in dye-sensitised solar cells (DSSCs) offers several advantages over using a single pigment. In this present study, natural dyes with different pigments were extracted from three local plants: Coccinia grandis (Ivy gourd leaves, IGL), Oryza sativa Linn (Black glutinous rice, BGR), and Curcuma longa L. (Turmeric, TM). Each colour extract absorbed various wavelengths of light. It was found that the single IGL-dye (green) had a greater light absorption and energy band gap over visible light than other extracts (dyes). Then combinations of these dyes were examined. A sensitised dye combination with a primary to secondary dye in a volumetric ratio of 80/20 exhibited multiple energy band gaps, implying multiple electron excitations at different photon energy levels. Compared to other mixed dyes, IGL/TM-dye had the highest absorbance and electron excitation at three wavelengths with the smallest energy band gap values of 1.74, 2.51, and 2.59 eV. The IGL-dye had the highest DSSC efficiency of 0.15 % for single dyes, followed by the TM-dye and BGR-dye, which had 0.12 % and 0.04 %, respectively. Interestingly, for combined dyes, the IGL/TM dye increased DSSC efficiency to 0.3 %. Since natural dyes tend to be less effective in DSSCs than synthetic dyes because they have a narrower absorption range, higher redox potentials, shorter operational lifetimes, higher rates of electron recombination, and different molecular structures, the dye co-sensitization strategy is one of the best ways to make more effective cells in the future.

1. Introduction

Renewable energy sources like water, the sun, wind, geothermal, and bioenergy are being explored to replace fossil fuels. The most exciting renewable energy source in tropical climates is solar. Silicon-based solar cells (single crystal, polycrystalline, and amorphous)

* Corresponding author. Centre for Alternative Energy Research and Development, Khon Kaen University, Thailand.
E-mail address: tanwon@kku.ac.th (T. Wongwuttanasatian).

https://doi.org/10.1016/j.heliyon.2023.e21533
Received 20 August 2023; Received in revised form 16 October 2023; Accepted 23 October 2023

are compound semiconductors, and third-generation solar cells (organics and DSSCs) are being developed [1,2]. Most solar cells convert sunlight into electricity at 12–17 % efficiency. The manufacturing process for crystalline silicon solar cells is difficult and environmentally harmful. DSSC was invented by O'Regan and Grätzel in 1988. Fig. 1 shows transparent conductive oxide, anode, cathode, semiconductor, electrolyte, and sensitised dye. DSSC has a low cost, a simple manufacturing method, and a large range of raw materials [3].

The four primary mechanisms of DSSC are dye excitation (photonic energy absorption), electron injection (transportation), oxidised-dye regeneration, and electrochemical reduction [4,5]. A photosensitive dye molecule on a metal oxide semiconductor absorbs incident light, exciting an electron from the highest occupied molecular orbital (HOMO) to the lowest unoccupied molecular orbital (LUMO) [6]. When dyes have LUMO energies greater than the conduction band (CB), excited electrons are injected into semiconductors [7]. The injected electron is transferred to the transparent conductive oxide and sent to an external circuit until it reaches the counter electrode, where it is retrieved and turned into electrical energy for a load. An electrolyte solution with an iodide/triiodide redox couple donates electrons to regenerate the oxidised dye. The oxidised dye molecules get new electrons from the redox mediator iodide ion (I^-), which is then oxidised to tri-iodide ions (I^{3-}) and moves to the DSSC counter electrode [8].

Many efforts have focused on sensitised dyes, which are essential to solar energy collection and conversion. Inorganic or metal complex sensitizers have excellent stability, light harvesting, and electron injection efficiency. Ruthenium-based metal complex photosensitizers like N3 (red dye), N719, and N749 are examples. However, complex synthesis procedures, expensive raw materials, environmental effects, a lack of biodegradability, and regulatory issues make treating inorganic dyes more expensive and problematic. Organic dyes or metal-free organic sensitisers have been employed to sensitise semiconductors due to their cost-effectiveness, wide molar adsorption coefficient, and controlled redox potential [9]. Using synthetic techniques, organic dyes can be synthesised in a lab for better control over their properties and performance. Natural pigments are excellent DSSC candidates despite their shorter absorption bands, greater energy levels (redox potential), inferior long-term stability, and higher electron recombination rate.

When exposed to UV rays from sunlight, natural colours degrade. Long-term UV exposure can cause photochemical reactions and structural changes in pigment molecules, reducing absorption efficiency and cell performance. Under the DSSC system's oxidative and reductive conditions, natural dyes may have poor electrochemical stability. Dye compounds undergo frequent redox reactions in DSSCs, which might cause side reactions, degradation, or unexpected cell reactions. These properties make DSSC less effective than synthetic dyes. However, photosensitive natural pigments are chosen for their abundance, sustainability, broad absorption range, aesthetic appeal, cultural value, and molecular engineering possibilities.

Various plant parts, including seeds [10], leaves [11–13], stalks [14], flowers [15], roots [16], curcumin [16], fruit skins [17,18], pokeweed [19], stalks [20], spinach leaves [6,21], and chlorophyll extracts [22]. Pheophytin (green, brown), chlorophyll (green), anthocyanin (purple), betalain (red, yellow), carotenoids (yellow), bixin (orange), astaxanthin (pink-red), and anthocyanin [10–12,14–18,23–29] absorb light at different wavelengths, resulting in varied peak absorption levels. Natural pigment extraction is easier than synthetic pigment production; usually, distilled or ionised water and ethanol are used as the extraction solvents. Due to the combination of each unique pigment, the colour extracted from various plants will vary, resulting in colours such as cream, pink, red, orange, purple, and black [27]. Usually, the effectiveness of natural dye sensitised-solar cells has been examined using titanium dioxide

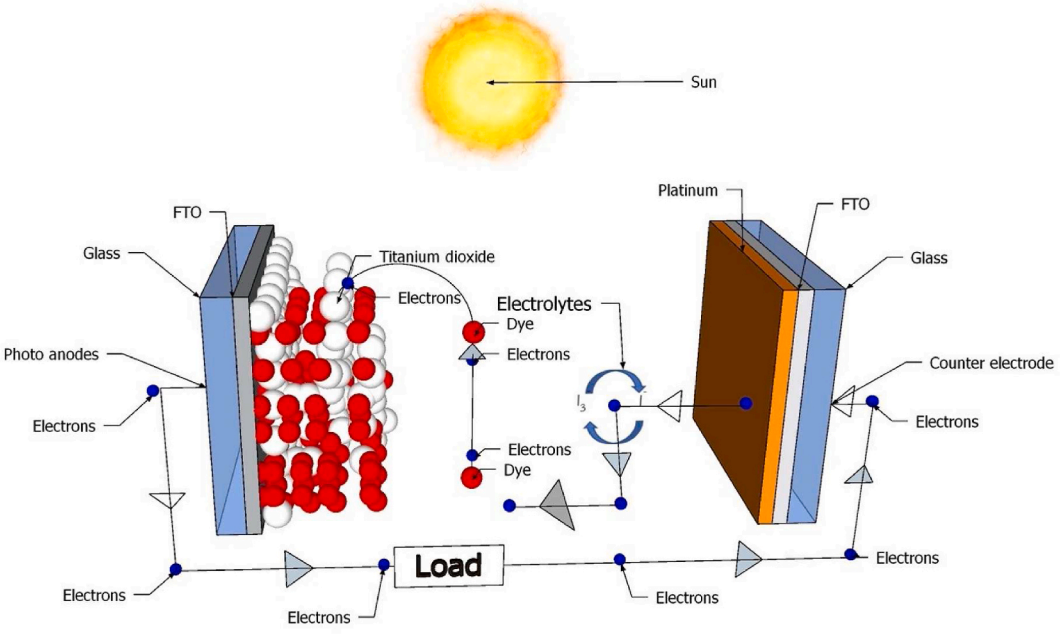

Fig. 1. DSSC component and light harvesting mechanism.

as counter electrodes and iodide/triiodide (I^-/I^{3-}) as electrolytes. Different natural dyes yield different cell performance. Note that cell efficiency can vary based on the sensitised dye, DSSC production methods, device architecture, testing conditions, experimental settings, and optimisation methodologies. For example, chlorophyll extracts gave varying DSSC efficiency values of 0.17 %, 0.13 %, 0.39 % and 0.40 % [6,13,16,18]. Anthocyanin photosensitized dyes obtained lower DSSC performance [17,28]. However, using anthocyanin-sensitised dye in Ref. [11] yielded greater DSSC efficiency than using chlorophyll-sensitised dye. Anthocyanin and isoquinoline alkaloid extracts from pokeweed stem resulted in the highest DSSC efficiency of 3.04 % [14]. According to Khalil E. Jasim et al. [16] and Hee-je Kim et al. [29], carotenoids-sensitised dye derived from curcumin gave DSSC efficiencies of 0.41 % and 0.60 %, respectively. Shalini Singh et al. [30] reported the best DSSC efficiency of 0.28 % from using anthocyanins and carotenoids as extracts.

Using a single colour led to low DSSC efficiency. Combining multiple dyes with different absorbance ranges can enhance dye properties for broader absorption and higher values, depending on the proportion of the extract and the type of pigment. There were consistent reports that the use of mixed extracts as a photosensitizing dye resulted in improved cell efficiency [8,11,31–38]. For instance, using combined anthocyanin (purple) and chlorophyll (green) dyes in different volume ratios improved DSSC performance, according to Hui Nan et al. [11], A.K. Swarnkar [33] and Pratiwi et al. [34]. Kabir et al. [35] discovered that combining turmeric dye (yellow) and red amaranth dye (anthocyanin) improved DSSC efficiency, similar to the combination of chlorophyll and vegetable anthocyanin [8]. Beetroot anthocyanin (red) and spinach chlorophyll (green) showed the highest DSSC efficiency, according to Bashar et al. [36]. Lastly, Ho Chang et al. [38] discovered that wormwood (chlorophyll) mixed with purple cabbage (anthocyanin) extracts increased DSSC efficiency.

Thus, natural pigments from various plants have been extracted for DSSC light sensitizers. Single pigments have limited absorption bands that may not match the sun's spectrum. Different pigments may be unstable in light or electrolytes. Using a combination of colours as sensitised dye in a DSSC increases the range of absorbed light and enhances dye stability, improving solar cell performance and longevity. Although numerous plants have been selected and studied to extract natural dyes for DSSC, it is beneficial to search for locally accessible, affordable, and abundant alternatives. In preliminary studies [39], sensitised pigments from ivy gourd leaves, black glutinous rice, and turmeric exhibited distinct light absorption properties; however, mixing colours improved light absorption. Consequently, the novelties of this work fall into the following points.

1. To completely examine the chemical components and characteristics of each natural dye obtained from ivy gourd leaves, black glutinous rice, and turmeric.
2. As proposed by the preliminary investigation, the combined-color dyes are utilised to assess DSSC performance (at 80:20 by vol).
3. The comparative analysis and discussion of the performance of Dye-Sensitised Solar Cells (DSSC) utilising single dyes and combination dyes are presented.
4. The utilisation of cost-effective and readily accessible natural dyes is suggested as an achievable alternative for fulfilling the requirements for the development of dye-sensitised solar cells (DSSC).

2. Materials and methods

2.1. Fabrication of combined-colour dyes DSSC

According to the previous research [39], the sensitised dyes extracted from Coccinia grandis (Ivy gourd leaves, IGL), Oryza sativa Linn (Black glutinous rice, BGR), and Curcuma longa L. (Turmeric, TM) were utilised to prepare multi-colour dyes. As it was reported that the light absorbance of the dye increased with concentration, the extraction of 30g of sample in 200 ml of ethanol was chosen to extract each single dye prior to mixing as bi-colour dyes in this study (seen in Fig. 2(a–c)). This investigation utilised EL-HPE light-performance electrolyte (SKU MS005615) and 18NR-T transparent titanium (TiO_2) paste (SKU MS2010). Transparent conductive glass plates SKU (MS001790) were made of fluorine-doped tin oxide (FTO), 7 Ω/sq, 100 mm × 100 mm x 2.2 mm. Ethyl alcohol (95 %, AR grade), Platinum (Pt) paste (Platisol T/SP) and Bemis Parafilm M PM992 wrapping film were utilised.

The FTO conductive glass was cut to a dimension of 2.5 cm × 2.5 cm and washed for 15 min in a sonicator bath containing a mixture

Fig. 2. The single dyes extracted from; (a) IGL (b) BGR and (c) TM.

of distilled water and ethanol (50:50 vol) and it was dried in the room atmosphere. In order to prepare the photoanode and counter electrode, the drawdown technique, which involves using a glass rod or similar tool to control the thickness, was used for the coating of TiO_2 and Pt on the clean FTO glass. A controlled amount of the titania paste or Pt paste was applied to the substrate using a pipette, then spread into a thin and uniform layer using the glass rod. In addition, conductive tape with a thickness of 0.02 mm was used to cover the top edge of the glass sheet to define the layer area and help control the thickness of the layer. The schematic of electrode preparation is presented in Fig. 3(a). So, the active material layer (coated with TiO_2 or Pt) was controlled at 2 cm × 2.5 cm with a thickness of 30 μm. Then, TiO_2/FTO glass was placed in a furnace at 450 °C for 30 min and allowed to cool for 24 h. Pt/FTO glass was annealed in a 450 °C furnace for 60 min and then cooled for approximately 24 h.

For the dye loading, the TiO_2/FTO glass was immersed in the prepared dye solution of 15 ml for 48 h to ensure that the entire active area of the substrate was covered by the solution. This allows the dye molecules to adsorb onto the surface of the TiO_2 particles, creating a thin dye layer. After that, the substrate was rinsed gently with ethanol to remove any unbound or excess dye molecules. The rinsed substrate was allowed to dry in an ambient condition to ensure complete drying and to avoid solvent remnants that may affect the performance and stability of the DSSC. Fig. 3(b) depicts the assembly characteristics of a DSSC in which the coated surface side of a sensitised TiO_2/FTO photoanode and a Pt/FTO counter electrode are in contact with each other. A paraffin sheet was used as spacer material along the edges of the photoanode to create a gap for the electrolyte. The spacer helps maintain the separation between the photoanode and counter electrode. The counter electrode was positioned above the photoanode, ensuring that the active areas aligned with each other. They were subsequently clamped together with clips, as shown in Fig. 3(c). Prior to measuring its efficiency, the electrolyte was introduced into the gap between them. The excess electrolyte was wiped away prior to sealing the cell edges with paraffin sheets to prevent electrolyte leakage.

Controlling electrode preparation, dye loading, and cell assembly ensures DSSC reproducibility. Properly store and handle materials, especially sensitive components like the dye, to prevent degradation. Fabrication also maintains stable temperature, humidity, and illumination.

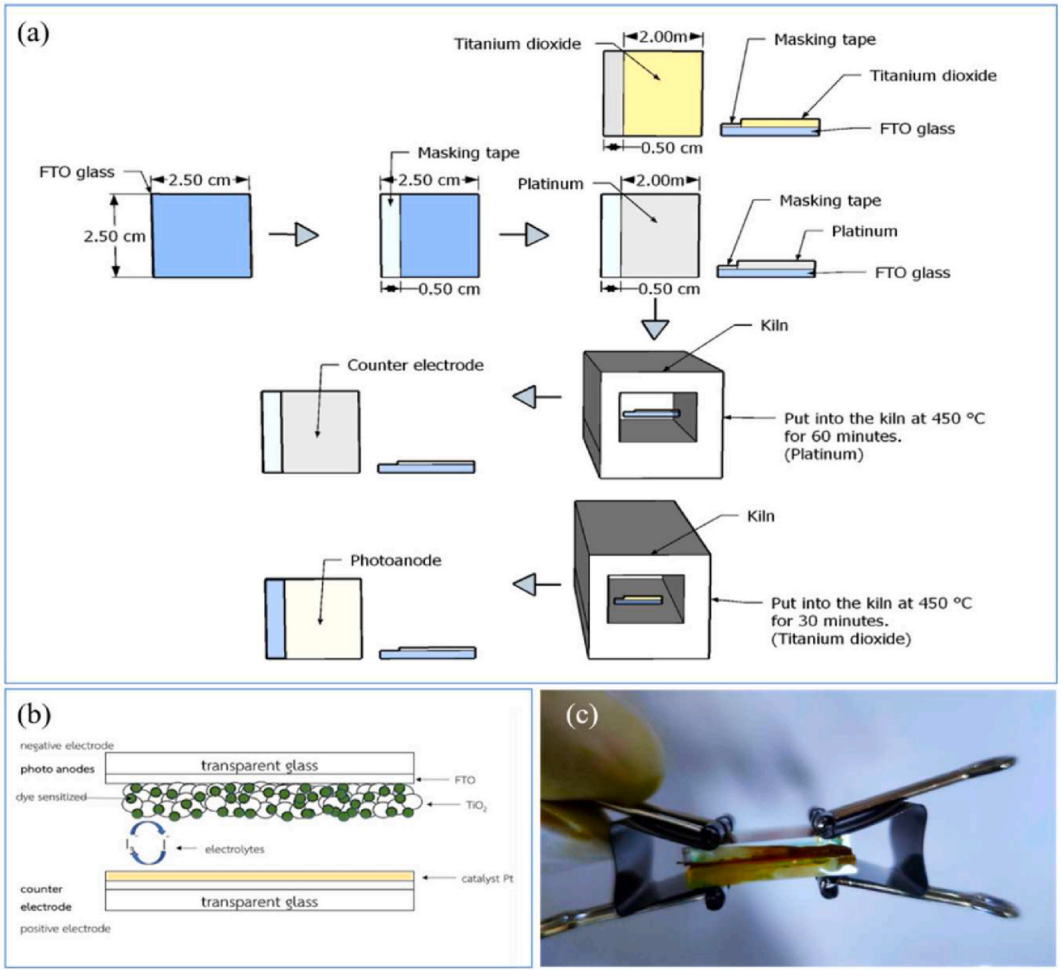

Fig. 3. (a) preparation step of photoanode and counter electrode, (b) schematic drawing of cell assembly and (c) ready fabricated DSSC cell for measurement.

2.2. Dye characterisation

Based on the absorption spectrometry data from the previous work [39], the best ratio of primary dye to secondary dye by volume for co-sensitised dyes was 80/20. In this report, a Fourier Transform Infrared Spectroscopy (FTIR) analyzer (NICOLET 6700) was utilised to further investigate the chemical structure of the single- and bi-extracted dyes. In this study, the samples were solid-state in FTIR. After putting the sample in the holder, the instrument is set up and the spectrum is measured. The light absorbances of these single and bicolor dyes were analysed using a UV–Vis spectrophotometer (SPECORD 200 plus). The dye solution is illuminated with visible light within the 400–800 nm wavelength range. As a baseline sample, ethanol of 95 % purity was used. The light absorbance characteristic curve enables the identification of colour pigment. The band gap energy of a sensitised dye describes the energy required to excite an electron from the highest occupied molecular orbital (HOMO) to the lowest unoccupied molecular orbital (LUMO). In order to anticipate the photophysical and photochemical properties of sensitizers, an accurate determination of the band gap energy is crucial. The band gap energies of IGL-dye, BGR-dye, TM-dye, and their mixtures have been determined using the relationship described in the study of H. Bashar et al. [36]. However, the goal of the present study is to look deeper into the relationship between the energy band gap and the structure of both single and combined dyes. Therefore, the UV–Vis spectrum can be used to calculate the band gaps of a material using the Tauc plot by plotting $(\alpha_0 h\nu)^{1/n}$ against photon energy $(h\nu)$. According to Eq. (1), the optical absorption strength is proportional to the difference between the photon energy and band gap [40].

$$(\alpha_0 h\nu)^{1/n} = B\left(h\nu - E_g\right)\left(eVcm^{-1}\right)^{1/n} \tag{1}$$

where h is the Planck's constant (6.625×10^{-34}Js or 4.135×10^{-15}eVs), ν is the photon's frequency (1/s), so that $h\nu$ is the energy of photon, E_g is the band gap energy (eV), and B is a proportionality constant. The value of the exponent n indicates the nature of the electronic transition. In most cases, the allowed transitions dominate the fundamental absorption processes, resulting in $n = 1/2$ or $n = 2$ for direct and indirect transitions, respectively. The linear coefficient of absorption, α_o is defined as the ratio of the decrease in incident beam energy to the wave's propagation distance within the material. The absorption coefficient is dependent on the energy of the incident photon and the length of the centre path of the absorbent and can be determined by Eq. (2) as follows:

$$\alpha_0 = 2.303 \times \frac{A}{t}\ (1/\mathrm{m}) \tag{2}$$

where A is the absorbance and t is the sample thickness. Consequently, the fundamental procedure for a Tauc analysis is to acquire optical absorbance data for the sample that covers a range of energies from below to above the band gap transition. Plotting $(\alpha_0 h\nu)^{1/n}$ versus $(h\nu)$ is a matter of testing $n = 1/2$ or $n = 2$ to compare which provides the better fit and thus identifies the correct transition type. The direct energy band gap (E_g) is subsequently determined using the X-intercept of this optimal plot.

Fig. 4. Solar simulator and DSSC testing.

2.3. Measurement of DSSC efficiency

The photoelectric conversion efficiencies were determined using simulated solar light (AM1.5, 1000 W/m^2), as shown in Fig. 4. The standard measurement conditions were the standard AM1.5G spectrum with a light intensity of 1000 W/m^2. The tested cell was placed on the support to be exposed to light, and a multimeter was used to record the current and the voltage in terms of short circuit current (I_{sc}), open circuit voltage (V_{oc}), maximum power current (I_{max}), maximum power voltage (V_{max}), fill factor (FF) and efficiency of dye sensitised solar cell (η). Three replicates of the identical DSSCs cells were generated and their efficiency values were analysed to obtain the mean and deviation values to ensure repeatability and reliability.

DSSC efficiency is defined as the ratio of energy output from the solar cell to solar energy incident on the solar cell, which can be calculated using Eq. (3).

$$\eta(\%) = \frac{V_{OC} \times J_{SC} \times FF}{P_{in}} \times 100 \tag{3}$$

The open circuit voltage (V_{oc}) is the voltage measured between two terminals with no load or current flowing. The short circuit current intensity (J_{sc}) is the short circuit current of the solar panel per unit area (A/m^2). P_{in} is the incident light intensity per unit area (W/m^2). Fill factor (FF) is the efficiency of solar energy that transfers power to a solar panel. So that FF is the ratio between the maximum power of an actual solar cell and the maximum power of an ideal solar cell. It can be calculated using Eq. (4).

$$FF = \frac{P_{\max}}{V_{oc} \times I_{sc}} \tag{4}$$

The maximal power output (P_{max}) is derived from the point on the I–V characteristics curve where the product of voltage and current is greatest. The P_{max} is calculated using the following relationships (Eq. (5)).

$$P_{\max} = V_{\max} I_{\max} \ (\mathrm{W}) \tag{5}$$

where I_{max} is the current at which the solar panel produces its maximum power. V_{max} is the voltage while solar panels are delivering maximal power. Therefore, the FF can be rewritten as follows in Eq. (6):

$$FF = \frac{V_{\max} \times I_{\max}}{V_{oc} \times I_{sc}} \tag{6}$$

3. Results and discussions

3.1. Chemical structure and light absorbance of dye extracts

The visible absorbance (400–700 nm) of a single dye has been analysed in the recent report [39]. IGL-dye (green) had the greatest absorption rate, whereas BGR-dye (purple) produced the lowest value. Each natural colour extract has a unique pigment structure;

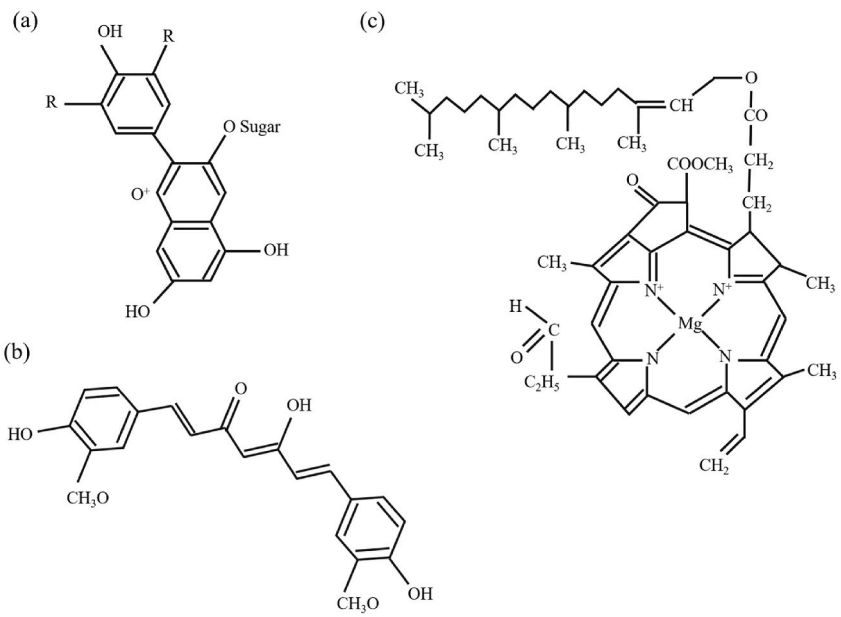

Fig. 5. The chemical structure of (a) Flavonoid (Anthocyanin), (b) Curcumin group and (c) chlorophyll.

consequently, their electrical properties vary when exposed to sunlight. Therefore, pigments are categorised according to their maximum absorbance of visible light. As stated in the introduction, natural dyes are categorised as anthocyanins, flavonoids, carotenoids, and chlorophyll. Green dye comprises chlorophyll, delphinidin, and cyanidin; yellow dye comprises carotenoids, aurone, chalcone, flavonol, and betaxanthin; and purple dye comprises carotenoids, cyanidin, and/or delphinidin [41]. Fig. 5 shows the basic structure of these pigments [42–44].

Natural flavonoid pigments can be classified according to their chemical structure as flavonols, flavones, flavanones, iso-flavones, catechins, anthocyanin, and chalcones. As shown in Fig. 5(a), flavonoid is composed of 15 carbon atoms, two phenyl rings, and three carbon bridges. The Anthocyanin group is a purple-red pigment found in flowers, fruits, leaves, and other plant elements including sprouts and roots [42]. Black glutinous rice contains anthocyanin pigment, which exhibits a broad region of the visible light spectrum. Due to the presence of carbonyl (C═O) and hydroxyl groups (OH) on its molecule, anthocyanin can bind to the surface of TiO_2 causing absorption in the low energy range. Consequently, dye-emitting electrons are transmitted to the conduction band of porous TiO_2 semiconductor film [45,46], which is advantageous to the photoelectric conversion effect. Turmeric-dye owes its characteristic yellow color to three major pigments; curcumin, demethoxy curcumin and bisdemethoxy curcumin [47]. Curcumin exhibits a keto-enol tautomerization [43], as shown in Fig. 5(b). It is an oil-soluble pigment, insoluble in water at acidic and neutral pH, but soluble in alkali. Ivy gourd leaves extract contains chlorophyll, a pigment found in the leaves of green plants, algae, and cyanobacteria. There are six pigment varieties in chlorophyll: chlorophyll-a, chlorophyll-b, chlorophyll-c1, chlorophyll-c2, and chlorophyll-f. The most common type is chlorophyll-a, which consists of a chlorine ring with a magnesium centre and various side chains and hydrocarbon traces [44], as shown in Fig. 5(c). Chlorophyll is the primary pigment in the photosynthetic system of plants. It is responsible for absorbing sunlight, converting solar energy into chemical energy, and conducting electron transfers. Chlorophyll is capable of absorbing red, blue, and violet wavelengths and reflecting them in green. The absorption peaks of chlorophyll in the visible region are typically located at 420 nm and 660 nm [45,46].

In the previous research [39], IGL, BGR and TM combined dyes were investigated with various primary dye to secondary dye (or P/S) ratios: 80/20, 60/40, 40/60 and 20/80 by volume. Based on the light absorbance of those mixed dyes, it has been suggested that a ratio of 80/20 should be used for DSSC sensitised dye. Consequently, IGL or TM was used as the primary dye in this present study, whereas TM or BGR was employed as the secondary dye. In a comparative study, TM/BGR-dye, IGL/TM-dye, and IGL/BGR-dye were used as sensitised dyes for DSSC. Therefore, a comparison of the absorbance at the 80/20 vol ratio of each dye mixture is shown in Fig. 6(a–c). It is evident that each dye mixture results in a different wavelength of absorption. According to the peaks, the extracted

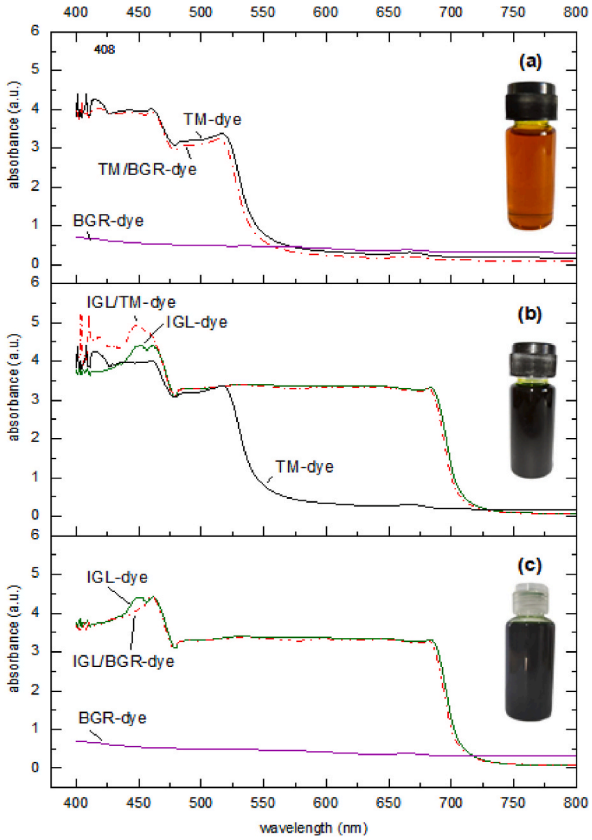

Fig. 6. Light absorption of natural single and co-sensitised dye of (a) TM/BGR-dye, (b) IGL/TM-dye and (c) IGL/BGR-dye at the ratio of 80/20 (% v/v).

dyes' absorption spectra intensities differed depending on their hue, transparency, and bandgap energies [48]. Compared to TM-dye and IGL-dye, BGR-dye has the lowest absorbance across the entire visible light spectrum, possibly caused by the use of ethanol as an extraction solvent. This result aligned with the findings reported by R. Syafinar [49]. BGR-dye (purple) has an absorption range of 400–500 nm with a maximum absorbance of 0.71 a.u. at 400 nm, which is comparable to the absorption spectrum reported by Sancun Hao [50]. Similar to Suyitno et al. [43], the yellow TM-dye has an absorption range of 400–530 nm. Its maximum absorption is 4.23 a.u. at 417 nm. IGL-dye (green) has an absorption range of 400–700 nm with a peak absorbance at 461 nm of 4.43 a.u. Also, the IGL-dye absorption spectrum is comparable to Hee-je Kim's report [29].

Due to the influence of the primary colour, the absorbance spectrum of the mixed pigment can be seen to be broader. A greater visible absorbance and a broader absorption spectrum are indicative of a dye's capacity to increase the possibility of solar energy photoelectrochemical conversion. BGR-dye (purple) has a lower absorbance at all light wavelengths than IGL-dye (green) and TM-dye (yellow). Therefore, when BGR-dye is used as a secondary dye, its impact on the light absorption of the blended dye is negligible. Nonetheless, the dye combination affects photoelectron excitation at distinct wavelengths due to the bonding of different colour structure components. Therefore, when the mixed sensitised dye is employed, the performance of the DSSC will be altered. It is necessary to evaluate the electron excitation energy at any wavelength of the sensitised dye in order to assure its suitability as a sensitised dye for DSSC.

The FTIR spectra of individual and co-sensitised dyes are shown in Fig. 7 (a) and (b), which reveals the structure of the existing function group. The TM-dye (yellow) spectrum exhibits broad spectra at 3346 cm^{-1}, which is attributed to the vibrations of the free hydroxyl-groups of phenol (Ar-OH) and alcohol (R–OH) [29,35]. Alkane C–H stretching occurs between 2975 and 2888 cm^{-1} [35]. The minor shoulder at 1646 cm^{-1} is attributed to carbonyl bond vibration (C═O) [29]. The C–O elongation is observed at 1452 and 1383 cm^{-1}, which corresponds to the vibrational modes of C–O elongation in the alcohol and phenol groups [29]. Also observed at 1383 cm^{-1} are C–N stretching and CO–*O*–CO vibration [35]. The bending vibrations of the C–H bond of alkene groups (RCH═CH_2) are observed at 960, 878, and 634 cm^{-1} [29], whereas the C═C stretching is observed at 877 cm^{-1} [35]. For the IGL-dye (green), spectra similar to those of the TM-dye appear in more detail. Broad spectra at 3346 cm^{-1} correspond to the vibrations of the free hydroxyl group of phenol (Ar-OH) and alcohol (R–OH) [36,38]. For the IGL-dye (green), similar spectra to those of the TM-dye are depicted with additional detail. Broad spectra at 3346 cm^{-1} is attributed to the free hydroxyl-group vibrations of phenol (Ar-OH) and alcohol (R–OH) [36,38]. The wavenumber of 2973 cm^{-1} corresponds to the O–H group [8] and the CH_3 vibration [36,38]. The wavelength at 2872 cm^{-1} has been associated with the N–H stretching [8] and C–H_2 [36,38]. The C═O vibration reveals itself at 1721 cm^{-1} [38]. The band at 1657 cm^{-1} is assigned to C═O [3] and C═C [36,38]. C–N vibration can also be detected at 1273 cm^{-1} [38]. The C–O vibration, C–*O*–C vibration and CH═CH_2 is detected at 1045, 1026, and 975 cm^{-1}, respectively [8,36,38]. There is an H-bond between molecules at 3418 cm^{-1}, a C═O stretching vibration at 1639 cm^{-1}, and a C–O–C stretching vibration at 1053 cm^{-1} [38]. Broad spectra at 3346 cm^{-1} correspond to vibrations of the free hydroxyl group of phenol (Ar-OH) and alcohol (R–OH) [24,35]. The C–H stretching corresponds to the wavenumbers 2975 and 2876 cm^{-1} [24]. The 1654 cm^{-1} band is assigned to the C═C [6], C═O [24] transitions. The bands at 1380 and 1333 cm^{-1} correspond to the C–N stretching and C–O stretching, respectively [35,36]. The band at 1045 cm^{-1} is assigned to the C–*O*–C ester bonds [8,24,38]. It can be observed that the transmittance values representing the functional groups of each dye are slightly different and that no new peak appears when they are used as a combination dye. This ensures that no new bonds are formed and no chemical reactions take place in the combined dye, but the transmittance intensity is altered slightly. Note that the presence of carbonyl and hydroxyl functional groups in the dye molecule affects the surface adherence of semiconducting TiO_2 photoanodes, making them promising for use as photosensitizers [51].

3.2. *Electron excitation of dye sensitiser*

The energy band gap is the optical band gap between the valence and conduction bands. The small energy band gap indicates that the distance between the valence band and the conduction band is narrow; consequently, electron transmission requires little energy. Despite the fact that the recent study [39] reported the energy band gap values for each dye, which were estimated based on its

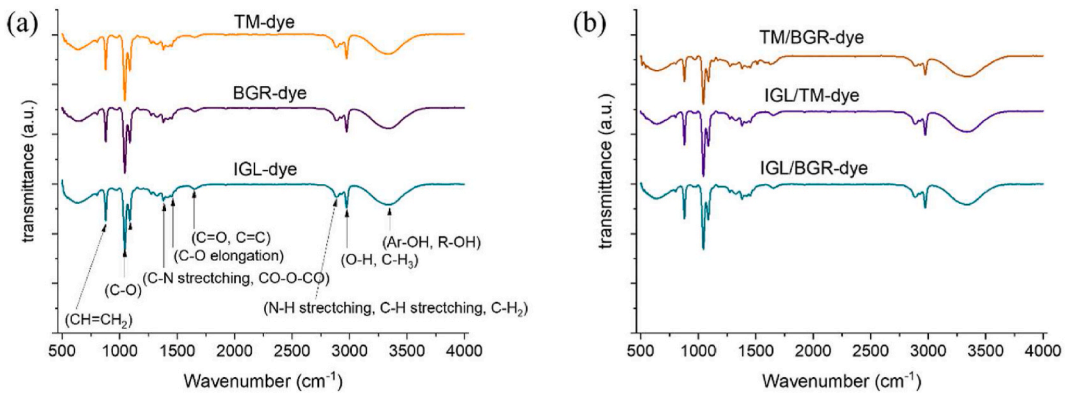

Fig. 7. FTIR spectra of (a) single-sensitised dyes extracted from TM, BGR and IGL, and (b) their combination at P/S of 80/20 by volume.

maximal absorbance wavelength (λ_{max}). However, to validate the absorbency of each dye in greater detail, in this report, absorbance as observed by the UV–Vis spectrum is utilised to compute the band gaps of dye using the Tauc Plot. Based on the plot of $(\alpha_0 h\nu)^{1/n}$ versus photon energy ($h\nu$) as expressed in Eq. (1), it has been found that the best fit to these data is achieved by employing the direct allowed transition (n = 1/2). As shown in Fig. 8, extrapolating the straight line towards lower photon energies yields the direct energy band gap (E_g) corresponding to the point of intersection with the vertical axis at the value of $(\alpha_0 h\nu)^2$ is zero.

Fig. 8 demonstrates that IGL-dye (green) has the smallest energy band gap of the three single dyes, with 1.74 eV, followed by TM-dye (yellow) with 2.28 eV, and BGR-dye (purple) with the highest value, 2.45 eV. The obtained E_g values differ slightly from the previous report [39], but the trend remains unchanged despite the use of different estimation methods. A large E_g value indicates that electrons are excited effectively at short wavelengths. Similarly, a low E_g value indicates that electron excitation at long wavelengths is effective. In addition, it has been observed that IGL-dye (green) electrons are excited at 713 and 494 nm, while TM-dye (yellow) electrons are excited at 544, 496, and 461 nm. Excitation of the electrons of IGL-dye (green) and TM-dye (yellow) at multiple wavelengths are likely caused by the combination of multiple pigments, resulting in multiple energy band gaps. In contrast, the electrons of the BGR-dye (purple) are excited at a singular wavelength of approximately 506 nm. Both IGL/BGR dye and IGL/TM dye are found to have the same minimum energy band gap of 1.74 eV. The similarities between the plot characteristics of IGL/BGR-dye and IGL-dye indicate that the pigment of BGR-dye has almost no effect on electron activation enhancement. It is conceivable that this mixed dye contains a low proportion of BGR-dye. Comparing the characteristic curve of IGL/TM-dye to that of IGL-dye, an additional energy band gap value of 2.59 eV is observed at 479 nm for electron excitation. This indicates that green and yellow dyes are harmonizing. The TM/BGR dye curve demonstrates that electrons are excited at the same three wavelengths as TM-dye. But there is a change in the electron excitation from 461 nm to a longer wavelength of 492 nm with an energy band gap of 2.52 eV.

The energy band gap of a DSSC dye controls the range of photons that dye molecules can absorb, which influences energy conversion efficiency and energy loss. The energy loss in a DSSC depends on dye molecule efficiency, cell design, and materials. Several innovative electron acceptors and redox mediators can optimise photon absorption and minimise energy losses by regulating the energy band gap, increasing open-circuit voltage and increasing DSSC efficiency. Zhaoyang Yao et al. [52] found that fine-tuning NB dye energy levels and steric configurations can significantly reduce energy losses in DSSCs.

Mixed dyes have multiple band gap energies, indicating that different photon energies excite electrons at each wavelength. The excited electrons are transferred to the holes, which demonstrates an n-type direct transition. Thus, the stimulated electrons transfer across the DSSC circuit. This suggests that the mixed dyes excite electrons at visible light wavelengths, transferring many electrons to the semiconductor. The circuit's electron mobility generates more electrical energy, making DSSC more efficient in converting light into electricity.

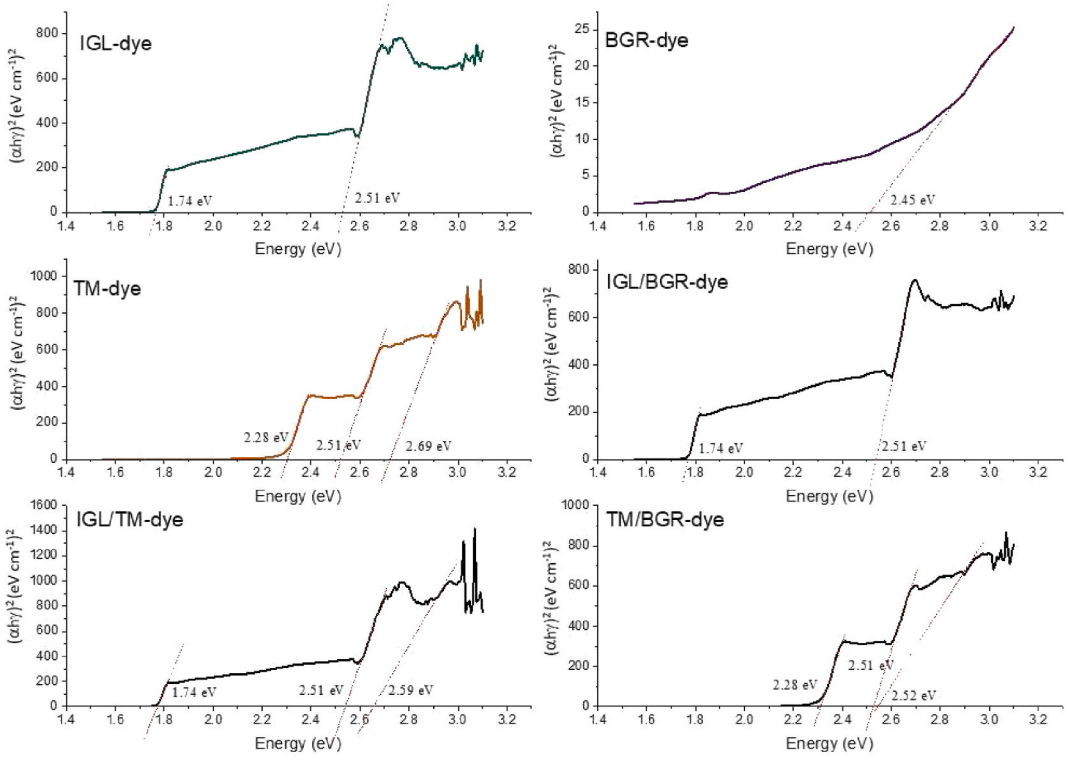

Fig. 8. Tuac plots of individual and co-sensitised dye.

3.3. Performance of natural dye sensitised solar cell

The morphology of the material is examined using scanning electron microscopy, which produces images with nanometer-level detail. Prior to TiO_2 coating, the FTO conductive glass had a rough surface, as shown in Fig. 9(a). After being coated with TiO_2, the FTO conductive glass surface is shown in Fig. 9(b) with small, evenly dispersed TiO_2 nanoparticles as a stable layer. On FTO glass, titania paste was applied with a controlled layer thickness of 0.03 mm. Redox ions and dye molecules can now more easily penetrate the TiO_2 film due to the development of a crystalline TiO_2 pore structure during annealing at 450 °C. A clear sintered layer was produced as a result. These nanoclusters provide a porous structure with a large surface area, enabling dye molecule adsorption [53,54]. It was found that an anode film structure with homogenous and mesoporous coatings along the substrate and no major craters is ideal for dye adsorption [54]. According to the related reports [48,55], the sintered nanosized TiO2 semiconductor was uniformly covered in FTO glass, and was well-connected with appropriate mesoporosity to form a wide electrolyte–electrode interface. These nanoclusters provide a porous structure with a large surface area, enabling dye molecule adsorption [53]. Dendrite shape with micrometer size of sintered Pt-coated, photocathode was also revealed [55] whereas other reports revealed the hierarchical morphology [48,53]. They confirmed that theirs Pt photocathode have excellent conductivity.

The relationship between the voltage applied across a DSSC and the current flowing through it, is represented by an I–V curve (measured using a solar light simulator). The performance of DSSC cells is affected by series resistance. Fig. 10 (a), I–V curve, shows the summary calculation for the DSSC eff. using Eqs. (3) and (6). The effectiveness of DSSC will be high if the blue area is equivalent to the gray area with high values of I_{sc} and V_{oc}. As shown in Fig. 10(b), IGL/BGR dye DSSC has lower I_{sc} and V_{oc} values than IGL-dye DSSC but higher values than BGR-dye DSSC. IGL-dye DSSC is discovered to be superior to IGL/BGR-dye DSSC and BGR-dye DSSC based on the order of the blue area beneath the graph. As shown in Fig. 10 (c), IGL/TM-dye DSSC has significantly higher I_{sc} and V_{oc} values than single dye DSSC. The blue area under the curve of IGL/TM-dye DSSC is the largest, followed by those of IGL-dye DSSC and TM-dye DSSC. As shown in Fig. 10 (d), TM/BRGR dye DSSC has a higher I_{sc} than single dye DSSC and a higher V_{oc} than BGR-dye DSSC but a marginally lower V_{oc} than TM-dye DSSC. The blue region under the I–V curve reveals that TM/BGR-dye DSSC is superior to TM-dye DSSC and BGR-dye DSSC. So that more blue areas under the graph will likely result in greater DSSC performance, as expected.

As depicted in Fig. 11, IGL-dye DSSC produces the highest I_{sc} and V_{oc} values, followed by TM-dye DSSC and BGR-dye DSSC. Short-circuit current is directly proportional to the amount of charge that can be generated and accumulated in a cell. It is essential to note that the short-circuit current is one of the most influential factors in determining the efficiency of a solar cell. Short-circuit photocurrent densities and open-circuit voltages are key parameters affecting cell efficiency [48]. The V_{oc} produced by IGL-dye DSSC is marginally greater than that of other dyes. The highest I_{sc} and the efficiency of the IGL-dye DSSC are 0.65 mA and 0.15 %, respectively. Following is the sequence of the FF values: BGR-dye DSSC > IGL-dye DSSC > TM-dye DSSC. At last, the DSSC efficiencies are determined to be IGL-dye DSSC (0.15 %) > TM-dye DSSC (0.12 %) > BGR-dye DSSC (0.04 %), corresponding to the absorbance and low energy band gap values described previously. Here, DSSC with BGR-dye has the lowest efficiency because its I_{sc} and V_{oc} values are the lowest.

Using mixed dyes result in IGL/TM dye DSSC with a greatest I_{sc} value of 1.45 mA, which is higher than TM/BGR dye DSSC and IGL/BGR dye DSSC, respectively. IGL/TM dye DSSC has a highest V_{oc} value of 0.55 V, whereas TM/BGR dye DSSC and IGL/BGR dye DSSC present comparable V_{oc} values. Although IGL/BGR dye DSSC has the maximum FF, IGL/TM dye DSSC is the most efficient at 0.30 %, with TM/BGR dye DSSC and IGL/BGR dye DSSC coming in second and third at 0.16 % and 0.10 %, respectively. It is found that IGL/BGR dye DSSC is less efficient than IGL-dye DSSC, which yields 0.15 %. Therefore, the combined use of IGL-dye and BGR-dye as a DSSC-sensitised dye is not advised, as BGR-dye has the lowest I_{sc} value, and its electrons are challenging to excite due to its high energy band gap. Consequently, the greater the value of I_{sc}, the greater the performance of DSSC.

It is noted that the data depicted in Fig. 11 are averaged values with small standard deviations (S.D.) shown as error bars.

Table 1 demonstrates that the I_{sc}, V_{oc} and FF values for DSSC vary depending on the dye. These findings relate to light harvesting

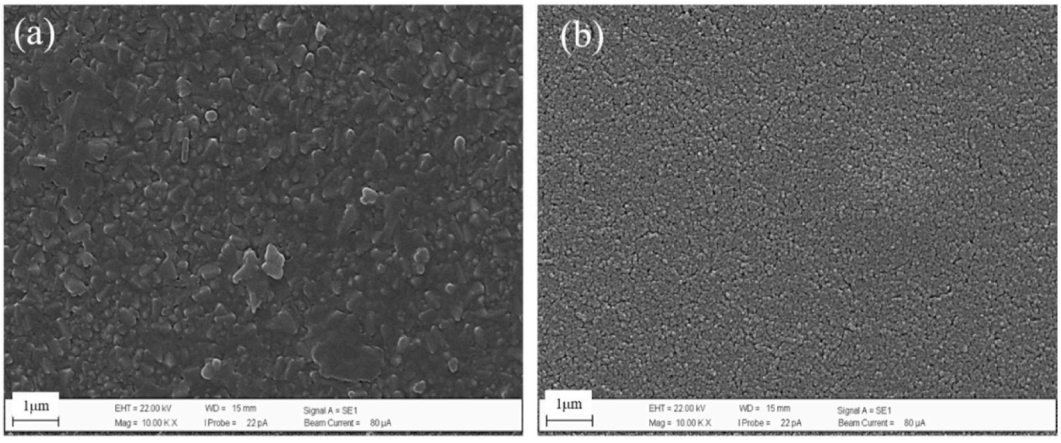

Fig. 9. SEM images of (a) FTO conductive glass and (b) TiO_2 coated-FTO conductive glass.

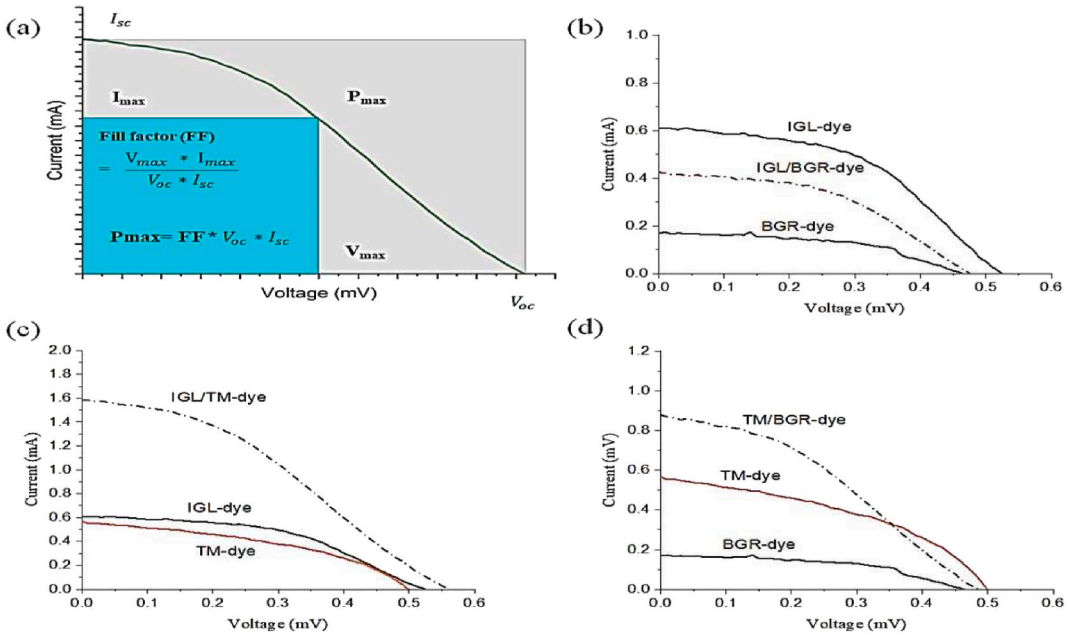

Fig. 10. I–V curves of (a) general DSSC, (b) IGL/BGR-dye DSSC, (c) IGL/TM-dye DSSC and (d) TM/BGR-dye DSSC.

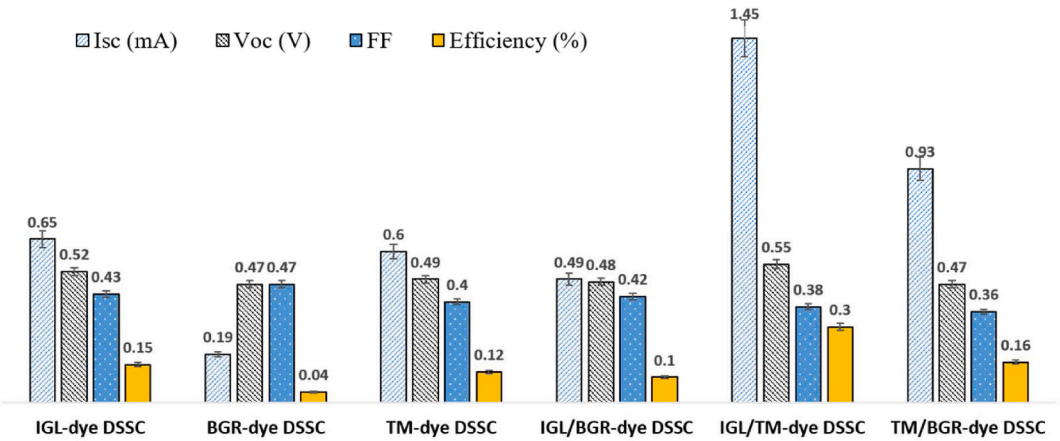

Fig. 11. Comparisons of DSSC data.

efficiency, dye pigment adsorption, dye molecule structure, electron injection, and photosensitized electrons, which impact photocurrent density [48,51]. The short circuit current of a dye-sensitised solar cell can vary based on a variety of factors, including the type and concentration of the dye, the composition and thickness of the photoelectrode, the intensity and spectral distribution of the incident light, and the operating temperature. The greater V_{oc} indicates that the electrolyte's energy level and LUMO energy level are sufficient to produce a high voltage difference.

As illustrated in Table 1, using IGL/TM-dye DSSC with a P/S ratio of 80/20, the efficiency is 0.30 %, whereas IGL-dye DSSC and TM-dye DSSC only gave 0.15 and 0.12 %, respectively. Similarly, using TM (yellow)/BGR (purple) yields a DSSC efficiency of 0.16 %, which is greater than using either TM (yellow) or BGR (purple) alone. This result is comparable to that of Ho Chang et al. [38], who discovered that a mixture of wormwood dye (green) and cabbage dye (purple) produced a DSSC efficiency of 1.29 %, which was greater than that of single cabbage dye (0.75 %) and single wormwood dye (0.53 %). In addition, the results of this present study are consistent with the findings of Sreeja and Pesala [37] that a mixture of spinach (green) and red spinach (red) yielded a DSSC efficiency of 0.601 %, which is greater than that of a single dye. Moreover, it is also in accordance with the findings of Maliheet Khalili et al. [24], who found that using mixed mulberry (purple)/saffron (yellow) dye resulted in a DSSC efficiency of 0.14 %, which was higher than that of using a single dye. According to the present report, however, IGL/TM-dye DSSC has shown greater efficiency than that of other reports [11,31,34,43,46,54,55]. The IGL/BGR-dye DSSC exhibits an efficiency of 0.10 %, which is higher than the single BGR-dye DSSC (0.04 %) but lower than the IGL-dye DSSC (0.15 %). IGL/BGR-dye DSSC performs significantly better than previous reports

Table 1
Comparison of photovoltaic performance of DSSC devices using natural sensitised dye.

Sensitised dye	I_{sc} (mA)	V_{oc} (V)	Fill Factor (FF)	Efficiency (%)	Ref.
IGL (green)	0.65	0.52	0.43	0.15	This work
Spinach (green)	0.41	0.59	0.59	0.17	[13]
Spinach (green)	0.35	0.44	0.49	0.36	[56]
Spinach (green)	2.875	0.347	0.468	0.466	[57]
BGR (purple)	0.19	0.47	0.47	0.04	This work
Black rice (purple)	0.010129	0.027	0.551	0.0001507	[46]
Blue pea flower (purple)	0.37	0.37	0.33	0.05	[31]
Alternanthera (purple)	0.9	0.58	0.60	0.31	[18]
Jabuticaba (purple)	0.38	0.41	0.29	0.13	[54]
TM (yellow)	0.60	0.49	0.40	0.12	This work
Curcumin (yellow)	0.577	0.633	0.507	0.185	[43]
Curcumin (yellow)	1.0055	0.5632	0.6399	0.36	[32]
Curcumin (yellow)	0.72	0.43	0.40	0.41	[58]
Peatals of Lantana repens (yellow)	0.45	0.69	0.34	0.12	[55]
Petals of Solidago canadensis flower (yellow)	0.93	0.79	0.42	0.31	[55]
Yellow Gerbera	1.22	0.59	0.53	1.54	[48]
IGL (Green)/TM (yellow)	1.45	0.55	0.38	0.30	This work
Green 20 % +Red 80 %	4.65	3.87	0.55	0.99	[57]
Spinach (green) + spinach (red)	1.25	0.53	0.68	0.601	[37]
TM (yellow) + BGR (Purple)	0.93	0.47	0.36	0.16	This work
Saffron(orange)50 %+Mulberry (purple)50 %	0.39	0.44	0.72	0.14	[24]
IGL (green) + BGR (purple)	0.49	0.48	0.42	0.10	This work
Green 50 % + Purple 50 %	1.13	0.46	0.46	0.154	[34]
2 anthocyanin: 5 chlorophylls	0.58	0.52	0.71	0.22	[11]
Green 50 %: Purple 50 %	3.16	0.66	0.62	1.29	[38]

of single-purple dye DSSC [31,46]. The combination of dyes has a positive effect on the DSSC's efficiency. Because each colour has a unique absorption rate, it can be said that when preparing mixed dyes, the appropriate mixing ratio, including the varieties of single dyes that are combined, must be taken into consideration. Be mindful that the dyes extracted from different parts of the same plant will have varied structural properties and light absorption behaviors. It is noted that the DSSC efficiencies attained for this project remained lower than those reported by others. It may be because the concentration of the extracted pigments varies by plant source, and the ratio of primary to secondary dyes does not remain constant.

According to the report of Nasim Sarwar et al. [59], the choice of metal oxide interlayers and electrode materials, along with the usage of natural photosensitive dyes as active mediators for light absorption in DSSCs, may affect cell performance. According to the study of Varsha Yadav et al. [60], they discovered that natural dyes have superior TiO_2 crystalline qualities than direct dyes, which led to DSSCs employing the fruit-based natural dye having higher power conversion efficiency. The immobilisation of dye molecules onto semiconducting metal oxide nanoparticles is critical for two reasons. Firstly, it enables the injection of electrons from the dye into the metal oxide's conduction band, ensuring electrical current generation. Secondly, it achieves a stable attachment of the dye which is essential for long-term device stability. Therefore, the creation and use of organic sensitizers with pyridine-containing anchoring moieties are typically associated with an increase in TiO_2 anchoring durability [61]. Therefore, the combination of Ivy gourd leaves (green) and Turmeric (yellow) dye at 80:20 by volume is an excellent source of dye for sensitization in this study.

4. Conclusions

Ivy gourd leaves, black glutinous rice, and turmeric yield IGL-dye (green), BGR-dye (purple), and TM dye (yellow) when extracted with ethanol at a ratio of 30 g of sample to 200 ml of ethanol, respectively. The single IGL-dye has a broader visible and near-infrared absorption spectrum than other dye extracts. The energy band gaps of dyes are ordered as 1.74, 2.28, and 2.45 eV for IGL-dye, TM-dye, and BGR-dye, respectively. For combined dyes, the IGL/TM dye, the TM/BGR dye, and the IGL/BGR dye, the volumetric ratio of primary dye to secondary dye is set at 80/20 based on the previous study [39]. The light absorbances of the single and mixed dyes are found to have peaks at different wavelengths. Moreover, the mixed-sensitised dye has multiple energy band gaps, implying multiple photoperiod excitations of electrons at different photon energy levels. At three different wavelengths, the energy band gaps of the IGL/TM dye are 1.74, 2.51, and 2.59 eV. For each single dye, the IGL-dye DSSC exhibits the highest efficiency of 0.15 %, followed by the TM-dye DSSC (0.12 %) and the BGR-dye DSSC (0.04 %). It is evident that using a bi-sensitised dye increases DSSC efficiency. Consequently, the efficiencies of IGL/TM dye DSSC, TM/BGR dye DSSC, and IGL/BGR dye DSSC are 0.30, 0.16, and 0.10 %, respectively. It can be concluded that the dye co-sensitization strategy is therefore one of the most effective techniques for the future development of cells with greater efficacy.

Moreover, it is advantageous to find locally accessible, inexpensive, and abundant alternatives. Regardless of whether the results are better or worse than previous research, this demonstrates the potential of local plants, as stated in the purpose of this study. Finally, in order to enhance the efficacy of DSSC, the development of natural photosensitive pigments from various plants should be continued. It is remarkable that the redox potential of the sensitising dye is necessary for the effective operation of charge transfer mechanisms. To facilitate efficient electron injection and regeneration, the redox potential of the dye and the redox potential of the electrolyte must be

appropriately matched. Additionally, electrochemical stability is essential for ensuring the long-term efficacy and durability of a device. To withstand exposure to light, moisture, and temperature, dye, electrolyte, and other components must be electrochemically stable. However, further research is recommended.

Funding

This research received no external funding.

Data availability Statement

Data will be made available on request.

CRediT authorship contribution statement

V. Seithtanabutara: Writing – review & editing, Writing – original draft, Supervision, Formal analysis. **N. Chumwangwapee:** Writing – original draft, Investigation, Data curation. **A. Suksri:** Writing – review & editing, Visualization. **T. Wongwuttanasatian:** Writing – review & editing, Visualization, Project administration, Methodology, Formal analysis, Conceptualization.

Declaration of competing interest

The authors declare that they have no known competing financial interests or personal relationships that could have appeared to influence the work reported in this paper.

Acknowledgments

The research team would like to thank the Center of alternative energy research and development, Khon Kaen University for supporting our work.

References

[1] Kumar Avinash Chandra, Sukhminder Singh Gill, Online, "Dye Sensitized Solar Films for Advanced and Effective Charge Collections" International Journal of Technology Research and Management ISSN 4 (10) (2017) 2348–9006. Paper ID: 2017/IJTRM/10/2017/9259.
[2] Kumar Avinash Chandra, Sukhminder Singh Gill, Recent progress in dye sensitized, Solar Cells" International Journal of Advance Research, Ideas and Innovations in Technology 3 (2017) 77–85.
[3] Geetam Richhariya, Bhim Charan Meikap, Anil Kumar, "Review on fabrication methodologies and its impacts on performance of dye-sensitized solar cells" Environmental, Science and Pollution Research 29 (2022) 15233–15251, https://doi.org/10.1007/s11356-021-18049-2.
[4] Jiawei Gong, Jing Liang, K. Sumathy, "Review on dye-sensitized solar cells (DSSCs): fundamental concepts and novel materials" Renewable and Sustainable, Energy Rev. 16 (8) (2012) 5848–5860, https://doi.org/10.1016/j.rser.2012.04.044. Nomenclature.
[5] Vipinraj Sugathan, Elsa John, K. Sudhakar, Recent improvements in dye sensitized solar cells, A review" Renewable and Sustainable Energy Reviews 52 (2015) 54–64, https://doi.org/10.1016/j.rser.2015.07.076.
[6] Haider Iftikhar, Gabriela Gava Sonai, Syed Ghufran Hashmi, Ana Flávia Nogueira, Peter David Lund, "Progress on electrolytes development in dye-sensitized solar cells" Materials 12 (12) (2019) 1998, https://doi.org/10.3390/ma12121998.
[7] C.O. Sreekala, I. Jinchu, K.S. Sreelatha, Yojana Janu, Narottam Prasad, Manish Kumar, Amit K. Sadh, M.S. Roy, Influence of solvents and surface treatment on photovoltaic response of dssc based on natural curcumin dye, IEEE J. Photovoltaics 2 (3) (2012) 312–319, https://doi.org/10.1109/JPHOTOV.2012.2185782.
[8] Kaustubh Patil, Soheil Rashidi, Hui Wang, Wei Wei, "Recent progress of graphene-based photoelectrode materials for dye-sensitized solar cells" International, Journal of Photoenergy Mar 26 (2019) 2019, https://doi.org/10.1155/2019/1812879.
[9] Sonu Kaliramna, Sardul Singh Dhayal, Rakhee Chaudhary, Sarita Khaturia, Keshav Lalit Ameta, Narendra Kumar, A review and comparative analysis of different types of dyes for applications in dye-sensitized solar cells, Braz. J. Phys. 52 (4) (2022) 136, https://doi.org/10.1007/s13538-022-01109-4.
[10] N.M. Gómez-Ortíz, I.A. Vázquez-Maldonado, A.R. Pérez-Espadas, G.J. Mena-Rejón, J.A. Azamar-Barrios, G. Oskam, "Dye-sensitized solar cells with natural dyes extracted from achiote seeds" Solar Energy Materials, Sol. Cell. 94 (1) (2010) 40–44, https://doi.org/10.1016/j.solmat.2009.05.013.
[11] Hui Nan, He Ping Shen, Gang Wang, Shou Dong Xie, Gui Jun Yang, Hong Lin, "Studies on the optical and photoelectric properties of anthocyanin and chlorophyll as natural co-sensitizers in dye sensitized solar cell" Optical Materials 73 (2017) 172–178, https://doi.org/10.1016/j.optmat.2017.07.036.
[12] Rajita Ramanarayanan, P. Nijisha, C.V. Niveditha, S. Sindh, "Natural dyes from red amaranth leaves as light-harvesting pigments for dye-sensitized solar cells" Materials Research, Bulletin 90 (2017) 156–161, https://doi.org/10.1016/j.materresbull.2017.02.037.
[13] Ahmed M. Ammar, Hemdan S.H. Mohamed, Moataz M.K. Yousef, Ghada M. Abdel-Hafez, Ahmed S. Hassanien, Ahmed S.G. Khalil, Dye-Sensitized Solar Cells (DSSCs) based on extracted natural dyes, J. Nanomater. 2019 (2019), https://doi.org/10.1155/2019/1867271. Article ID 1867271, 10 pages.
[14] Emre Güzel, Barış Seçkin Arslan, Veysel Durmaz, Mert Cesur, Ömer Faruk Tutar, Tuğba Sarı, Mehmet İşleyen, Mehmet Nebioğlu, İlkay Şişman, Photovoltaic performance and photostability of anthocyanins, isoquinoline alkaloids and betalains as natural sensitizers for, DSSCs" Solar Energy 173 (2018) 34–41, https://doi.org/10.1016/j.solener.2018.07.048.
[15] Ishwar Chandra Maurya, Shalini Singh, Pankaj Srivastava, Biswajit Maiti, Lal Bahadur, Natural dye extract from Cassia fistula and its application in dye-sensitized solar cell, Experimental and density functional theory studies" Optical Materials 90 (2019) 273–280, https://doi.org/10.1016/j.optmat.2019.02.037.
[16] Abdel-Latif, S. Monzir, B. Mahmoud, Abuiriban, M. Taher, El-Agez, Sofyan A. Taya, Dye-sensitized solar cells using dyes extracted from flowers, leaves, parks, and roots of three trees, Int. J. Renew. Energy Resour. 5 (1) (2015) 294–298.
[17] M.C. Ung, C.S. Sipaut, J. Dayou, K.S. Liow, J. Kulip, R.F. Mansa, Fruit based dye sensitized, Solar Cells" Materials Science and Engineering 217 (1) (2017), 012003, https://doi.org/10.1088/1757-899X/217/1/012003.
[18] Mahmoud A.M. Al-Alwani, Norasikin A. Ludin, Abu Bakar Mohamad, Abd Amir H. Kadhum, Abduljabbar Mukhlus, "Application of dyes extracted from Alternanthera dentata leaves and Musa acuminata bracts as natural sensitizers for dye-sensitized solar cells" Spectrochimica, Acta Part A: Molecular and Biomolecular Spectroscopy 192 (2018) 487–498, https://doi.org/10.1016/j.saa.2017.11.018.

[19] Emre Güzel, Barış Seçkin Arslan, Veysel Durmaz, Mert Cesur, Ömer Faruk Tutar, Tuğba Sarı, Mehmet İşleyen, Mehmet Nebioğlu, İlkay Şişman, Photovoltaic performance and photostability of anthocyanins, isoquinoline alkaloids and betalains as natural sensitizers for DSSCs, Sol. Energy 173 (2018) 34–41, https://doi.org/10.1016/j.solener.2018.07.048.

[20] Xiao-Feng Wang, Arihiro Matsuda, Yasushi Koyama, Hiroyoshi Nagae, Shin-ichi Sasaki, Hitoshi Tamiaki, Yuji Wada, Effects of plant carotenoid spacers on the performance of a dye-sensitized solar cell using a chlorophyll derivative: enhancement of photocurrent determined by one electron-oxidation potential of each carotenoid, Chem. Phys. Lett. 423 (4–6) (2006) 470–475, https://doi.org/10.1016/j.cplett.2006.04.008.

[21] Hitoshi Tamiaki, Norihisa Hagio, Shinsaku Tsuzuki, Yuxiao Cui, Taisuke Zouta, Xiao-Feng Wang, Yusuke Kinoshita, Synthesis of carboxylated chlorophyll derivatives and their activities in dye-sensitized solar cells, Tetrahedron 74 (30) (2018) 4078–4085, https://doi.org/10.1016/j.tet.2018.06.017.

[22] Xiao-Feng Wang, Osamu Kitao, Haoshen Zhou, Hitoshi Tamiaki, Shin-ichi Sasaki, Extension of π-conjugation length along the Q y axis of a chlorophyll a derivative for efficient dye-sensitized solar cells, Chemical communications 12 (2009) (2019) 1523–1525, https://doi.org/10.1039/B820540J.

[23] Giuseppe Calogero, Jun-Ho Yum, Alessandro Sinopoli, Gaetano Di Marco, Michael Grätzel, Mohammad Khaja Nazeeruddin, "Anthocyanins and betalains as light-harvesting pigments for dye-sensitized solar cells" Solar, Energy 86 (5) (2012) 1563–1575, https://doi.org/10.1016/j.solener.2012.02.018.

[24] Malihe Khalili, Mohammad Abedi, Hossein Salar Amol, "Influence of saffron carotenoids and mulberry anthocyanins as natural sensitizers on performance of dye-sensitized solar cells" Ionics 23 (2017) 779–787, https://doi.org/10.1007/s11581-016-1862-3.

[25] A. Orona-Navar, I. Aguilar-Hernández, A. Cerdán-Pasarán, T. López-Luke, M. Rodríguez-Delgado, D.L. Cárdenas-Chávez, E. Cepeda-Pérez, N. Ornelas-Soto, "Astaxanthin from Haematococcus pluvialis as a natural photosensitizer for dye-sensitized solar cell" A. Orona-Navar et al, Algal Res. 26 (2017) 15–24, https://doi.org/10.1016/j.algal.2017.06.027.

[26] Nandarapu Purushothamreddy, Reshma K. Dileep, Ganapathy Veerappan, M. Kovendhan, D. Paul Joseph, "Prickly pear fruit extract as photosensitizer for dye-sensitized solar cell" Spectrochimica, Acta Part A: Molecular and Biomolecular Spectroscopy 228 (2020), 117686, https://doi.org/10.1016/j.saa.2019.117686.

[27] S. Shalini, R. Balasundara Prabhu, S. Prasanna, Tapas K. Mallick, S. Senthilarasu, "Review on natural dye sensitized solar cells: operation, materials and methods" Renewable and Sustainable, Energy Rev. 51 (2015) 1306–1325, https://doi.org/10.1016/j.rser.2015.07.052.

[28] D.D. Pratiwi, F. Nurosyid, A. Supriyanto, R. Suryana, Optical properties of natural dyes on the dye-sensitized solar cells (DSSC) performance, J. Phys. Conf. 776 (1) (2016), 012007, https://doi.org/10.1088/1742-6596/776/1/01200.

[29] Hee-je Kim, Dong- Jo Kim, S.N. Karthick, K.V. Hemalatha, C Justin Raj, "Curcumin efficient dye-sensitized solar cells" int, J. Electrochem. Sci. 8 (63) (2013) 8320–8328, https://doi.org/10.1016/S1452-3981(23)12891-4.

[30] Shalini Singh, Ishwar Chandra Maurya, Shubham Sharma, Shiva Prakash Singh Kushwaha, Pankaj Srivastava, Lal Bahadur, "Application of new natural dyes extracted from Nasturtium flowers (Tropaeolum majus) as photosensitizer in dye-sensitized solar cells" International, Journal for Light and Electron Optics 243 (2021), 167331, https://doi.org/10.1016/j.ijleo.2021.167331.

[31] Khwanchit Wongcharee, Vissanu Meeyoo, Sumaeth Chavadej, "Dye-sensitized solar cell using natural dyes extracted from rosella and blue pea flowers" Solar Energy Materials, Sol. Cell. 91 (7) (2007) 566–571, https://doi.org/10.1016/j.solmat.2006.11.005.

[32] Geetam Richhariya, Anil Kumar, Fabrication and characterization of mixed dye, Natural and synthetic organic dye" Optical Materials 79 (2018) 296–301, https://doi.org/10.1016/j.optmat.2018.03.056.

[33] A.K. Swarnkar, Sanjay Sahare, Nikhil Chander, Rajesh K. Gangwar, S.V. Bhoraskar, Tejashree M. Bhave, Nanocrystalline titanium dioxide sensitised with natural dyes for eco-friendly solar cell application, J. Exp. Nanosci. 10 (13) (2015) 1001–1011, https://doi.org/10.1080/17458080.2014.951410.

[34] D.D. Pratiwi, F. Nurosyid, K.A. Supriyanto, R. Suryana, Performance improvement of dye-sensitized solar cells (DSSC) by using dyes mixture from chlorophyll and anthocyanin, J. Phys. Conf. 909 (1) (2017), 012025, https://doi.org/10.1088/1742-6596/909/1/012025.

[35] F. Kabir, M.M.H. Bhuiyan, M.R. Hossain, H. Bashar, M.S. Rahaman, M.S. Manir, R.A. Khan, T. Ikegami, Improvement of efficiency of dye sensitized solar cells by optimizing the combination ratio of natural red and yellow dyes, International Journal for Light and Electron Optics 179 (2019) 252–258, https://doi.org/10.1016/j.ijleo.2018.10.150.

[36] H. Bashar, M.M.H. Bhuiyan, M.R. Hossain, F. Kabir, M.S. Rahaman, M.S. Manir, T. Ikegami, Study on combination of natural red and green dyes to improve the power conversion efficiency of dye sensitized solar cells, International Journal for Light and Electron Optics 185 (2019) 620–625, https://doi.org/10.1016/j.ijleo.2019.03.043.

[37] S. Sreeja, B. Pesala, Co-sensitization aided efficiency enhancement in betanin–chlorophyll solar cell, Materials for Renewable and Sustainable Energy 7 (25) (2018) 1–14, https://doi.org/10.1007/s40243-018-0132-x.

[38] Ho Chang, Mu Jung Kao, Tien Li Chen, Chih Hao Chen, Kun Ching Cho, Xuan Rong Lai, "Characterization of natural dye extracted from wormwood and purple cabbage for dye-sensitized solar cells" International, Journal of Photoenergy 2013 (2013) 8. Article ID 159502.

[39] N. Chumwangwapee, A. Suksri, T. Wongwuttanasatian, Investigation of Bi-colour, Natural Dyes Potential for Dye Sensitized Solar Cell" Energy Reports 9 (2023) (2022) 415–421, https://doi.org/10.1016/j.egyr.2023.05.132.

[40] Patrycja Makuła, Michał Pacia, Wojciech Macyk, How to correctly determine the band gap energy of modified semiconductor photocatalysts based on, UV-Vis Spectra" The Journal of Physical Chemistry Letters 9 (23) (2018) 6814–6817, https://doi.org/10.1021/acs.jpclett.8b02892.

[41] Glennise Faye C. Mejica, Rameshprabu Ramaraj, Yuwalee Unpapraom, Natural dye (chlorophyll, anthocyanin, carotenoid, flavonoid) photosensitizer for dye-sensitized solar cell, A review" Maejo International Journal of Energy and Environmental Communication 4 (1) (2022) 12–22, https://doi.org/10.54279/mijeec.v4i1.247970.

[42] Oluwaseun Adedokun, Kamil Titilope, Ayodeji Oladiran Awodugba, Review on natural dye-sensitized solar cells (DSSCs), International Journal of Engineering Technologies IJET 2 (2) (2016) 34–41, https://doi.org/10.19072/ijet.96456.

[43] Suyitno, Yuda Virgantara Agustia, Lullus Lambang Govinda Hidajat, Budi Kristiawan, Atmanto Heru Wibowo, "Effect of light and temperature on the efficiency and stability of curcumin-dye-sensitized solar cells" International Energy, Journal 18 (1) (2018) 53–60.

[44] Sancun Hao, Jihuai Wu, Yunfang Huang, Jianming Lin, "Natural dyes as photosensitizers for dye-sensitized solar cell" Solar Energy 80 (2) (2006) 209–214, https://doi.org/10.1016/j.solener.2005.05.00.

[45] Norasikin A. Ludin, A.M. Al-Alwani Mahmoud, Abu Bakar Mohamad, Abd Amir H. Kadhum, Kamaruzzaman Sopian, Nor Shazlinah Abdul Karim, "Review on the development of natural dye photosensitizer for dye-sensitized solar cells" Renewable and Sustainable, Energy Rev. 31 (2014) 386–396, https://doi.org/10.1016/j.rser.2013.12.001.

[46] Rathanawan Magaraphan, Jaruwan Joothamongkhon, "Performance of Dye-Sensitized Solar Cells Using ZnO-Natural Dyes from Sappan Wood, Noni Leaves, Safflower and Black Rice" Advanced Materials Research, vol. 658, 2013, pp. 25–29, https://doi.org/10.4028/www.scientific.net/amr.658.25.

[47] L. Péret-Almeida, A.P.F. Cherubino, R.J. Alves, L. Dufossé, M.B.A. Glória, Separation and determination of the physico-chemical characteristics of curcumin, demethoxycurcumin and bisdemethoxycurcumin" Food Research International 38 (8–9) (2005) 1039–1044, https://doi.org/10.1016/j.foodres.2005.02.021.

[48] F.M.M. Dos Santos, A.M.B. Leite, L.R.B. da Conceição, Y. Sasikumar, R. Atchudan, M.F. Pinto, R. Suresh Babu, A.L.F. de Barros, "Effect of bandgap energies by various color petals of Gerbera jamesonii flower dyes as a photosensitizer on enhancing the efficiency of dye-sensitized solar cells" Journal of Materials Science, Materials in Electronics 33 (25) (2022) 20338–20352, https://doi.org/10.1007/s10854-022-08849-8.

[49] R. Syafinar, N. Gomesh, M. Irwanto, M. Fareq, Y.M. Irwan, Potential of purple cabbage, coffee, blueberry and turmeric as nature based dyes for dye sensitized solar cell (DSSC), Energy Proc. 79 (2015) 799–807, https://doi.org/10.1016/j.egypro.2015.11.569.

[50] Sancun Hao, Jihuai Wu, Yunfang Huang, Jianming Lin, "Natural dyes as photosensitizers for dye-sensitized solar cell" Solar Energy 80 (2) (2006) 209–214, https://doi.org/10.1016/j.solener.2005.05.009.

[51] F.C. Ferreira, R.S. Babu, A.L. de Barros, S. Raja, L.R. da Conceição, L.H. Mattoso, "Photoelectric performance evaluation of DSSCs using the dye extracted from different color petals of Leucanthemum vulgare flowers as novel sensitizers" Spectrochimica, Acta Part A: Molecular and Biomolecular Spectroscopy 233 (2020), 118198, https://doi.org/10.1016/j.saa.2020.118198.

[52] Zhaoyang Yao, Yaxiao Guo, Linqin Wang, Hao Yan, Yu Guo, Daniele Franchi, Fuguo Zhang, Lars Kloo, Licheng Sun, Energy-loss reduction as a strategy to improve the efficiency of dye-sensitized solar cells, Sol. RRL 3 (10) (2019), 1900253, https://doi.org/10.1002/solr.201900253.

[53] B.C. Ferreira, D.M. Sampaio, R.S. Babu, A.L. De Barros, Influence of nanostructured TiO_2 film thickness in dye-sensitized solar cells using naturally extracted dye from, Thunbergia erecta flowers as a photosensitizer" Optical Materials 1 (86) (2018) 239–246, https://doi.org/10.1016/j.optmat.2018.10.016.
[54] D.M. Sampaio, R.S. Babu, H.R. Costa, A.L. De Barros, Investigation of nanostructured TiO 2 thin film coatings for DSSCs application using natural dye extracted from, jabuticaba fruit as photosensitizers" Ionics 1 (25) (2019) 2893–2902, https://doi.org/10.1007/s11581-018-2753-6.
[55] B.C. Ferreira, R.S. Babu, L.R. da Conceição, H.O. da Cunha, D.M. Sampaio, L.M. Samyn, A.L. de Barros, Performance evaluation of DSSCs using naturally extracted dyes from petals of Lantana repens and Solidago canadensis flowers as light-harvesting, units" Ionics 28 (11) (2022) 5233–5242, https://doi.org/10.1007/s11581-022-04727-9.
[56] R. Syafinar, N. Gomesh, M. Irwanto, M. Fareq, Y.M. Irwan, Chlorophyll pigments as nature based dye for dye-sensitized solar cell (DSSC), Energy Proc. 79 (2015) 896–902, https://doi.org/10.1016/j.egypro.2015.11.584.
[57] Khalil Ebrahim Jasim, Seamas Cassidy, Feryad Zaki Henari, Akil Aziz Dakhel, "Curcumin Dye-Sensitized Solar Cell" Journal of Energy and Power Engineering 11 (2017) 409–416, https://doi.org/10.17265/1934-8975/2017.06.006.
[58] F. Kabir, M.M.H. Bhuiyan, M.S. Manir, M.S. Rahaman, M.A. Khan, T. Ikegami, Development of dye-sensitized solar cell based on combination of natural dyes extracted from Malabar spinach and red spinach, Results Phys. 14 (2019), 102474, https://doi.org/10.1016/j.rinp.2019.102474.
[59] Nasim Sarwar, Monas Shahzad, Rabia Ghaffar, Khalid Javed, Mahroze Munam, Aneel Pervez, Abdul Ghaffar, Fabrication of DSSC based on Capsicum annuum and Tamarindus indica plant seeds extract as natural photosensitizers, Sol. Energy 257 (2023) 314–323, https://doi.org/10.1016/j.solener.2023.04.039.
[60] Varsha Yadav, Chandra Mohan Singh Negi, D. Kishore Kumar, Saral Kumar Gupta, Fabrication of eco-friendly, low-cost dye sensitized solar cells using harda fruit-based natural dye, Opt. Mater. 122 (2021), 111800, https://doi.org/10.1016/j.optmat.2021.111800.
[61] Gianna Reginato, Massimo Calamante, Lorenzo Zani, Alessandro Mordini, Daniele Franchi, Design and synthesis of organic sensitizers with enhanced anchoring stability in dye-sensitized solar cells, Pure Appl. Chem. 90 (2) (2018) 363–376, https://doi.org/10.1515/pac-2017-0403.